HHS Public Access

Author manuscript

ACS Nano. Author manuscript; available in PMC 2016 June 27.

Published in final edited form as:

ACS Nano. 2015 ; 9(4): 4475–4483. doi:10.1021/acsnano.5b01074.

Ultrasensitive Rapid Detection of Human Serum Antibody Biomarkers by Biomarker-Capturing Viral Nanofibers

Yicun Wang[#†], **Zhigang Ju**[#‡,†], **Binrui Cao**[‡], **Xiang Gao**[†], **Ye Zhu**[‡], **Penghe Qiu**[‡], **Hong Xu**[‡], **Pengtao Pan**[†], **Huizheng Bao**[§], **Li Wang**[*,†], and **Chuanbin Mao**[*,‡]

[†]Institute of Genetics and Cytology, School of Life Sciences, Northeast Normal University, 5268 Renmin Street, Changchun, Jilin Province 130024, P.R. China

[‡]Department of Chemistry & Biochemistry, Stephenson Life Sciences Research Center, University of Oklahoma, 101 Stephenson Parkway, Norman, Oklahoma 73019-5300, United States

[§]Jilin Provincial Tumor Hospital, Changchun, Jilin Province 130021, P.R. China

[#] These authors contributed equally to this work.

Abstract

Candida albicans (*C. albicans*) infection causes high mortality rates within cancer patients. Due to the low sensitivity of the current diagnosis systems, a new sensitive detection method is needed for its diagnosis. Toward this end, here we exploited the capability of genetically displaying two functional peptides, one responsible for recognizing the biomarker for the infection (antisecreted aspartyl proteinase 2 IgG antibody) in the sera of cancer patients and another for binding magnetic nanoparticles (MNPs), on a single filamentous fd phage, a human-safe bacteria-specific virus. The resultant phage is first decorated with MNPs and then captures the biomarker from the sera. The phage-bound biomarker is then magnetically enriched and biochemically detected. This method greatly increases the sensitivity and specificity of the biomarker detection. The average detection time for each serum sample is only about 6 h, much shorter than the clinically used gold standard method, which takes about 1 week. The detection limit of our nanobiotechnological method is approximately 1.1 pg/mL, about 2 orders of magnitude lower than that of the traditional antigen-based method, opening up a new avenue to virus-based disease diagnosis.

[*]Address correspondence to: cbmao@ou.edu, wangli@nenu.edu.cn. .

Conflict of Interest: The authors declare no competing financial interest.

Supporting Information *Available:* Production of polyclonal anti-Sap2-IgG in rabbits to be used for determining detection limit, determination of the limit of detecting anti-Sap2-IgG by using recombinant Sap2 protein and our ASIT-MNP-phage as biomarker-capturing probes in ELISA, the sequencing results of selected phage clones, Western blot for PK-ASIT-phage and wild-type phage with candidiasis serum, ELISA result of the purified anti-Sap2-IgG solutions with a series of dilutions, and Western blotting analysis of anti-Sap2-lgG. This material is available free of charge *via* the Internet at http://pubs.acs.org.

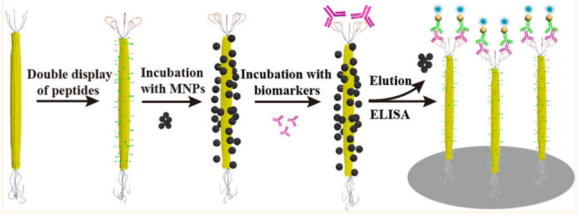

Keywords

fungal infection; nanoparticles; nanofibers; viruses; peptides

Invasive fungal infection is a major cause of increased mortality in cancer patients.[1–10] About 70%–87% of such infection is caused by *Candida* species,[11–13] especially *Candida albicans* (*C. albicans*) (50%–67%).[14–20] *C. albicans* can cause bloodstream infection (candidaemia) and/or organ infection (disseminated candidiasis) in immunocompromised individuals such as cancer patients.[21,22] Both candidaemia and disseminated candidiasis lead to high mortality rates of cancer patients.[23] To reduce such high mortality, it is important to diagnose *C. albicans* infection and initiate antifungal therapy early.[3,9,24] However, the blood culture method, the current gold standard in the clinical diagnosis[25] of *C. albicans* infection, takes about 5 days[26] to get reliable results,[27] resulting in the delay of antifungal therapies.[27–29] On the other hand, other techniques, *e.g.*, enzyme-linked immunosorbent assay (ELISA) for the detection of specific proteins related to *C. albicans* infection,[30–32] cannot efficiently detect the low levels of marker proteins generated at the early stage of *C. albicans* infection, such as antisecreted aspartyl proteinase 2 IgG (anti-Sap2-IgG).[30,33–36] Therefore, a new strategy with high time-efficiency and sensitivity is needed for the early detection of anti-Sap2-IgG.

Phage, as a nontoxic virus, has recently emerged as a new analytical platform.[37–39] Hence we used fd phage functionalized with both anti-Sap2-IgG-targeting (ASIT) peptide (VKYTS, an epitope of Sap2, which we found to be able to capture anti-Sap2-IgG[30]) and MNPs to facilitate the capture (by ASIT peptide) and enrichment (by MNPs) of the anti-Sap2-IgG from serum, followed by the detection of the biomarker by ELISA (Scheme 1). The fd phage (~900 nm long and 7 nm wide)[40,41] is a nanofiber-like virus composed of coat proteins surrounding a ssDNA genome that encodes these proteins,[42] including ~4000 copies of a major coat protein (called pVIII) constituting the side walls and 5 copies each of four minor coat proteins (termed pIII, pVI, pVII, and pIX) forming the two tips.[43] When DNA encoding peptides are inserted into the genes of the coat proteins, the peptides are displayed at the tips of the phage by fusion to minor coat proteins and/or along the side walls by fusion to pVIII.[40] This allows us to codisplay two peptides on a single viral nanofiber, including an ASIT peptide at one tip (as fusion to pIII), which allows the phage to selectively capture anti-Sap2-IgG in sera, and an MNP-binding peptide (identified by phage display in this work) along the side walls (as fusion to pVIII), which enables the decoration of the phage with MNPs for magnetically enriching the captured anti-Sap2-IgG (Scheme 1). The resultant phage (termed as ASIT-MNP-phage) can greatly increase the sensitivity for detecting anti-Sap2-IgG in sera from cancer patients by ELISA analysis.

RESULTS AND DISCUSSION

Water-soluble Fe_3O_4 MNPs (~5 nm in diameter), a magnetic label used for enriching specific molecules,[44] were synthesized following a reported protocol[45] and confirmed by transmission electron microscopy (TEM, Figure 1a), magnetic enrichment (Figure 1a inset) and X-ray diffraction (XRD, Figure 1b). MNP-binding peptides were identified from a phage-displayed random peptide library (f88-15mer library, a gift from Dr. George P. Smith at the University of Missouri) by biopanning against the synthesized MNPs following our published protocol (Figure 2a).[46] We used the pVIII-based phage library instead of the commonly used pIII-based library for two main reasons. First, we want the MNPs to be bound to the side wall of phage (constituted by ~4000 copies of pVIII) by the MNP-binding peptides displayed and the MNP-binding peptides are expected to bind MNPs more efficiently when displayed on the side wall of phage in the same way as when they are selected during biopanning. Second, more candidate peptides are displayed on the side wall than at the tip (made of 5 copies of pIII) of an individual viral nanofiber, leading to more efficient target binding by a phage nanofiber in the pVIII library than in a pIII library during the affinity-selection process.

To start biopanning process, the f88-15mer phage library, which is made of billions of phage clones with each clone displaying a 15-mer peptide on the side wall (pVIII), was allowed to interact with a microcentrifuge tube to remove phages that were bound with the tube. The resultant depleted phage library was used as an input to interact with MNPs placed in a microcentrifuge tube. A magnet was then applied to attract the MNPs along with MNP-binding phages to the bottom of the tube and the supernatant containing nonbinding phages was discarded. The MNP-phage pellet was then washed 5 times with a washing buffer to get rid of weak MNP-binding phages and the strong MNP-binding phages were eluted using an elution buffer, amplified and used as a new input for the next round of selection. After a binding-washing-elution process was repeated three times, 62 phage clones with high MNP-binding affinity were randomly picked up and sent for DNA sequencing. The sequencing results (Supporting Information Table S1) show that 2 sequences have 4 repeats, 1 sequence has 3 repeats, 7 sequences have 2 repeats, and 37 sequences only have 1 repeat. Therefore, we picked the 10 sequences with more than 1 repeat (Supporting Information Table S1) for the binding-affinity tests to find out the best MNP-binding phage/peptide. In the binding-affinity tests, 10 phage clones were separately amplified and titered, and the same amount of each phage nanofiber (3.5×10^8 plaque forming units (pfu)) was allowed to interact with excess MNPs. After 5 rounds of washing, the MNP-binding phage nanofibers were eluted, titered and counted. The phage displaying the best MNP-binding peptide should have the highest number of bound phage particles. The results (Figure 2b) show that the phage displaying the peptide PTYSLVPRLATQPFK (termed as PK peptide) had the highest number of bound phage nanofibers (3.24×10^8 pfu), indicating this PK peptide is the best MNP-binding peptide.

The PK peptide and our reported ASIT peptide (VKYTS)[30] were then displayed on the side wall (pVIII) and at the tip (pIII) of phage, respectively (Scheme 1a), forming PK-ASIT-phage. Briefly, the DNA sequences encoding the PK and ASIT peptides were respectively inserted into the specific sites of the genes of pVIII and pIII in the phagemid f388-55. The

recombinant f388-55 phagemid was then transformed into *Escherichia coli* MC1061 to produce bioengineered phage, which displays PK peptide on its side wall (pVIII display) and ASIT peptide at its tip (pIII display) (Scheme 1a). Then, the anti-Sap2-IgG-targeting and MNP-binding abilities of the PK-ASIT-phage were tested. Western blot results (Supporting Information Figure S1) show that only PK-ASIT-phage with the pIII displaying ASIT peptide can target anti-Sap2-IgG, while the wild type (WT) phage cannot, confirming the biomarker-binding ability of PK-ASIT-phage. Next, the binding between 100 μg MNPs and different amounts of PK-ASIT-phage was studied (Figure 2c). The results showed that with the increase of the added phage from 7.5×10^9 to 4.8×10^{11} pfu, the number of bound phage nanofibers increased from 7.2×10^9 to 4.5×10^{11} pfu, indicating PK-ASIT-phage could efficiently bind with MNPs in PBS buffer. But when the added phage was over 4.8×10^{11} pfu, the bound phage remained as ~4.5×10^{11} pfu, suggesting all the binding peptides displayed on PK-ASIT-phage were occupied by MNPs and confirming 4.5×10^{11} pfu is the maximum amount of PK-ASIT-phage for binding with 100 μg MNPs. Therefore, 4.5×10^{11} pfu of PK-ASIT-phage and 100 μg MNPs were mixed to form ASIT-MNP-phage complexes.

After the mixing of PK-ASIT-phage and MNPs, ASIT-MNP-phage complexes were formed (Figure 1c,d), in which MNPs were assembled along PK-ASIT-phage. The specificity of the ASIT-MNP-phage complexes was then studied. In the specificity test, ASIT-MNP-phage complexes capturing anti-Sap2-IgG from the sera of cancer patients were collected by a magnet (Scheme 1b) and then the phage-bound anti-Sap2-IgG was eluted off MNPs using an elution buffer for Western blot analysis. It should be noted that the elution buffer was the same as that used to remove MNP-binding phage away from the MNPs during biopanning (Figure 2a). The Western blot results (Figure 3a) indicate that anti-Sap2-IgG was specifically captured and detected by ASIT-MNP-phage from the sera of the *C. albicans*-infected cancer patients (instead of from the sera of the healthy control), confirming the specificity of ASIT-MNP-phage against anti-Sap2-IgG.

The high sensitivity of using our ASIT-MNP-phage complexes for detecting anti-Sap2-IgG was confirmed by plotting the predesigned concentrations of anti-Sap2-IgG, produced and validated through an immunological method (Supporting Information Figures S2 and S3), *versus* the experimentally determined ELISA signal (Figure 3b,c). The detection limit of our ASIT-MNP-phage method was found to be as low as 1.1 pg/mL, 2 orders of magnitude lower than that of rSap2-based method (89.56 pg/mL) (Supporting Information). In addition, the average detection time for each sample is only about 6 h, much shorter than the clinically used blood culture method (~5 days[26]).

The ASIT-MNP-phage complexes were then used to detect human anti-Sap2-IgG in sera from cancer patients clinically diagnosed with *C. albicans* infection by the blood culture method. 68 serum samples from *C. albicans*-infected cancer patients and 144 serum samples from healthy control were collected and analyzed using our ASIT-MNP-phage-based method (Scheme 1). ASIT-phage and rSap2 were used as control detection probes. A cutoff value is defined as the mean plus 3 times standard deviations (SDs) of the absorbance values in the ELISA analysis of these 144 control sera.[47] When the absorbance in ELISA was higher than the cutoff value, the samples were considered infection-positive. By applying this criteria to independent tests, 65 ± 1 out of 68 serum samples from *C. albicans*-infected

cancer patients were detected as infection-positive, whereas only 30 ± 2 and 33 ± 2 samples were detected by ASIT-phage and rSap2 methods, respectively (Table 1 and Figure 4a). These results indicate that the sensitivity of our ASIT-MNP-phage method (95.6% (= [(65/68) × 100%])) was much higher than those from the control methods of ASIT phage (44.1% (=[(30/68) × 100%])) and rSap2 (48.5% (=[(33/68) × 100%])). When ASIT-MNP-phage was applied to detect 144 serum samples from healthy control, only 3 samples were detected as infection-positive (false positive) (Table 1). The detection specificity of ASIT-MNP-phage method reached ~97.9% (=(144–3)/144 × 100%), a little higher than that of ASIT phage (97.2%) and rSap2 (91.7%) methods. Therefore, our ASIT-MNP-phage method showed a much higher sensitivity and a little higher specificity for detecting *C. albicans* infections within cancer patients than the rSap2 and ASIT-phage methods.

In addition, we also independently studied the sensitivity of our method in detecting *C. albicans* infections in patients with different cancer types, including lung (21 samples), breast (19 samples), intestinal (7 samples), and other (21 samples) cancer (Table 2 and Figure 4b). The ELISA results (Figure 4b) show that the sensitivity of our ASIT-MNP-phage method was much higher [95.2% (lung cancer), 94.7% (breast cancer), 100.0% (intestinal cancer), and 95.2% (other cancer types)] in comparison with ASIT-phage method [57.1% (lung cancer), 52.6% (breast cancer), 42.9% (intestinal cancer), and 23.8% (other cancer types)] and rSap2 method [57.1% (lung cancer), 57.9% (breast cancer), 47.1% (intestinal cancer), and 28.6% (other cancer types)]. These results suggest that ASIT-MNP-phage can be used to detect *C. albicans*-infected patients of different cancer types.

Our results showed that ASIT-MNP-phage method outperformed ASIT phage and rSap2 methods in detecting human anti-Sap2-IgG. The key to such success lies in the use of magnetic virus (*i.e.*, ASIT-MNP-phage) (Scheme 1). Namely, ASIT-MNP-phage enabled the biomarkers to be magnetically enriched first and then biochemically analyzed. For ASIT phage and rSap2 methods, although both ASIT phage and rSap2 can capture anti-Sap2-IgG with high specificity, they could not enrich the captured anti-Sap2-IgG by means of a magnet. This fact explains why our ASIT-MNP-phage method showed much higher detection sensitivity but a little higher specificity than ASIT phage and rSap2 methods. Furthermore, circulating viruses, which act as antigens, are expected to bind target antibodies more efficiently in a solution phase, resulting in more efficient capturing of the antibodies and better detection limit than the conventional ELISA method. The orientation of the antigens, the peptides displayed on the viruses, may also be one of the factors that contribute to the higher capturing efficiency in our method as the antigen orientation is important in detecting target antibody.[48] In addition, nanotechnology-based antibody detection was usually tested on the laboratory or animal samples.[49] Here, we directly tested the virus-based method on the infected cancer patients (68 samples). The high sensitivity of our ASIT-MNP-phage method may benefit the early detection of *C. albicans* infection in the cancer patients in intensive care unit. Moreover, our virus-based method is not limited to the detection of anti-Sap2-IgG. Because a peptide that can target other biomarkers can be identified using phage display,[46,50,51] our method can be developed as a general method for detecting biomarkers with high sensitivity and specificity.

CONCLUSIONS

In conclusion, we identified a MNP-binding peptide, PTYSLVPRLATQPFK and double-displayed this peptide and a reported anti-Sap2-IgG-targeting peptide, VKYTS,[30,52] on fd phage to form PK-ASIT-phage. Then we constructed the magnetic virus by binding the phage with MNPs and confirmed its high stability, specificity, and sensitivity. Finally, we used the magnetic virus to detect the anti-Sap2-IgG in sera from *C. albicans*-infected cancer patients, and found our magnetic virus-based method is much more sensitive than using viruses or antigens alone and takes much shorter time than the clinical gold standard. Our method can serve as a general strategy for detecting other biomarkers with high sensitivity and specificity because biomarker-binding peptides can be identified by phage display and displayed on the surface of phage.

METHODS

Affinity-Selection of Fe_3O_4 MNP-Binding Phage Clones

We selected the MNP-binding phage clones by following our previously published protocol with minor revision.[46] Specifically, 0.2 mg of Fe_3O_4 MNPs was resuspended in 100 μL of binding buffer (100 μL TBS with 0.1% (w/w) Tween 20). An f88-15mer phage library (~2×10^{12} phage) was diluted in 1 mL of binding buffer and the mixture was allowed to interact with a microcentrifuge tube first to remove phages that were bound to the tube materials. The resultant phage library was allowed to interact with MNPs in a microcentrifuge tube for 2 h at 37 °C. A magnet was then applied to attract the MNPs along with MNP-bound phage to the bottom of the tube and the supernatant containing nonbinding phages was discarded. The MNP-phage pellet was washed five times by repeating the process of resuspension in 1 mL of washing buffer (TBS with 0.1% Tween 20) and the subsequent centrifugation to remove the supernatant. The bound phages were eluted from MNPs with 500 μL of elution buffer (0.1 N HCl, and pH adjusted to 2.2 with glycine) for 7 min on a shaker. The eluate was neutralized by mixing it with 35 μL of 1 M Tris-HCl (pH = 9.1) immediately. The entire first-round eluate was amplified by infecting starved *E. coli* K91 BlueKan cells,[46] and the amplified phages were then purified with a double polyethylene glycol (PEG) precipitation method. The purified phages were used as a new input library and the selection procedure as the first round was repeated. After the third round of selection, the eluted phages were not amplified. Instead, the neutralized eluates were titered and 62 colonies were randomly picked up for DNA sequencing.

Construction of PK-ASIT Phage by Phage Double Display Technique

To insert VKYTS sequence into the gene of pIII of phage, an f388-55 RF phage vector was first double digested by *BglI* (Takara, Japan) and then ligated with the adaptor molecule created by annealing two oligonucleotides (5′-tcgtcaaatatacttctactg-3′; 5′-tagaagtatatttgacgacgt-3′) encoding the epitope VKYTS by using T4 DNA ligase (Takara, Japan). The recombinant plasmid (f388-55-VKYTS) was then transformed into competent *E. coli* MC1061 cells. The positive clones with gene insertion in the phage vector verified by polymerase chain reaction (PCR) were selected for sequencing to confirm the correct insertion of the gene encoding VKYTS. The transformed *E. coli* MC1061 cells were

cultured in a shaking incubator at 37 °C overnight to amplify the recombinant plasmid, which was isolated by using a QIAprep Spin Miniprep Kit from Qiagen. To insert PTYSLVPR-LATQPFK sequence (termed PK peptide) into the gene of pVIII of the phage, the recombinant plasmid was double digested by *Pst*I and *Hind*III (Takara, Japan) and then ligated with the gene segment encoding the peptide PTYSLVPRLATQPFK. The resultant double-recombinant phage vector (f388-55-VKYTS-PK) was transformed into the competent *E. coli* MC1061 cells. The positive clones with gene insertion in the phage vector verified by PCR were further selected for sequencing to confirm the correct insertion of the genes encoding VKYTS and PK peptide. The transformed cells were incubated in a shaking incubator at 37 °C overnight to produce PK-ASIT-phage nanofibers. The phage nanofibers were precipitated and purified by double PEG method.

Serum

A total of 68 *C. albicans*-infected cancer patients were enrolled in this study. Those patients were treated at China-Japan Union Hospital of Jilin University, Changchun, Jilin. All patients were given informed consent prior to the collection of their serum samples, and the samples were stored at −80 °C until assayed. The sera from 144 healthy volunteers were kindly provided by Northeast Normal University Affiliated Hospital. Serum samples from a panel of the 144 healthy volunteers were used to determine the cutoff value of the ELISA methods for the detection of the anti-Sap2 antibody. All cases have been analyzed by clinicians.

ELISA Tests for the Detection of Anti-Sap2-IgG Antibody from Serum by ASIT-MNP-Phage Method

A volume of 800 μL of diluted serum samples was incubated with the ASIT-MNP-phage complexes formed due to the binding interaction between 100 μg MNPs and 4.5×10^{11} pfu of PK-ASIT-phage for 1 h. After incubation, ASIT-MNP-phage complexes, which had captured the anti-Sap2-IgG antibody from serum, were collected and enriched by a magnet and then the MNPs were eluted off ASIT-MNP-phage by using 100 μL of the elution buffer and 15 μL of a neutralization buffer (1 M Tris-HCl, pH = 9.1). MNPs were magnetically removed by a magnet and the phage-bound anti-Sap2-IgG in the remnant solution was coated onto a 96-well plate in 115 μL of carbonate buffer (pH 9.6) for 2 h at 37 °C. Next, the plate was blocked with phosphate-buffered saline (PBS) buffer (containing 1% BSA). Then the blocking buffer was discarded. A horseradish peroxidase (HRP)-labeled goat-anti-human IgG (diluted in 1:5000) solution was subsequently added to the wells of the plate and incubated for 45 min. Finally, the unbound HRP-labeled goat-anti-human IgG was removed and 3, 3′, 5, 5′-tetramethylbenzidine (TMB) peroxidase substrate solution was added to the plate, followed by incubation for 15 min. The reaction of converting the TMB substrate into a blue product by HRP was stopped by the addition of 2 M H_2SO_4, and the absorbance of the resultant yellow product was measured with ELISA reader (Thermo) at 450 nm. All samples were run in triplicate. If the measured OD_{450nm} of one serum sample was higher than the average OD_{450nm} of the 144 serum samples from healthy people plus 3 times of standard deviation,[47] this serum sample was considered as *C. albicans*-infected.

Supplementary Material

Refer to Web version on PubMed Central for supplementary material.

Acknowledgment

Y.W., Z.J., X.G., P.P., H.B., L.W. and C.B.M. would like to thank the grants from the National Natural Science Foundation of China (81028010 and 81373231), Jilin Provincial Government of the People's Republic of China (20130727034YY) and the Ministry of Science and Technology of the People's Republic of China (2014DFA31740). Z.J., B.R.C., P.H.Q., Y.Z., H.X. and C.B.M. would also like to thank the financial support from National Science Foundation (CMMI-1234957, DMR-0847758 and CBET-0854465), National Institutes of Health (1R21EB015190), Department of Defense Peer Reviewed Medical Research Program (W81XWH-12-1-0384), Oklahoma Center for the Advancement of Science and Technology (HR14-160) and Oklahoma Center for Adult Stem Cell Research (434003).

REFERENCES AND NOTES

1. Xu XL, Lee RT, Fang HM, Wang YM, Li R, Zou H, Zhu Y, Wang Y. Bacterial Peptidoglycan Triggers *Candida albicans* Hyphal Growth by Directly Activating the Adenylyl Cyclase Cyr1p. Cell Host Microbe. 2008; 4:28–39. [PubMed: 18621008]
2. Beaussart A, Alsteens D, El-Kirat-Chatel S, Lipke PN, Kucharikova S, Van Dijck P, Dufrene YF. Single-molecule Imaging and Functional Analysis of Als Adhesins and Mannans During *Candida albicans* Morphogenesis. ACS Nano. 2012; 6:10950–10964. [PubMed: 23145462]
3. Sipsas NV, Kontoyiannis DP. Invasive Fungal Infections in Patients with Cancer in the Intensive Care Unit. Int. J. Antimicrob. Agents. 2012; 39:464–471. [PubMed: 22337064]
4. Cheng SC, Joosten LAB, Kullberg BJ, Netea MG. Interplay between *Candida albicans* and the Mammalian Innate Host Defense. Infect. Immun. 2012; 80:1304–1313. [PubMed: 22252867]
5. Kadosh D, Lopez-Ribot JL. *Candida albicans*: Adapting to Succeed. Cell Host Microbe. 2013; 14:483–485. [PubMed: 24237692]
6. Safdar A, Chaturvedi V, Cross EW, Park S, Bernard EM, Armstrong D, Perlin DS. Prospective Study of Candida Species in Patients at a Comprehensive Cancer Center. Antimicrob. Agents Chemother. 2001; 45:2129–2133. [PubMed: 11408236]
7. Anderson LM, Krotz S, Weitzman SA, Thimmapaya B. Breast Cancer-Specific Expression of the *Candida albicans* Cytosine Deaminase Gene Using a Transcriptional Targeting Approach. Cancer Gene Ther. 2000; 7:845–852. [PubMed: 10880014]
8. Wilcock BC, Endo MM, Uno BE, Burke MD. C2′-OH of Amphotericin B Plays an Important Role in Binding the Primary Sterol of Human Cells But Not Yeast Cells. J. Am. Chem. Soc. 2013; 135:8488–8491. [PubMed: 23718627]
9. Liu R, Chen X, Falk SP, Mowery BP, Karlsson AJ, Weisblum B, Palecek SP, Masters KS, Gellman SH. Structure-Activity Relationships Among Antifungal Nylon-3 Polymers: Identification of Materials Active Against Drug-Resistant Strains of *Candida albicans*. J. Am. Chem. Soc. 2014; 136:4333–4342. [PubMed: 24606327]
10. Steinbach WJ, Reedy JL, Cramer RA Jr. Perfect JR, Heitman J. Harnessing Calcineurin As a Novel Anti-Infective Agent against Invasive Fungal Infections. Nat. Rev. Microbiol. 2007; 5:418–430. [PubMed: 17505522]
11. Peman J, Zaragoza R. Current Diagnostic Approaches To Invasive Candidiasis In Critical Care Settings. Mycoses. 2010; 53:424–433. [PubMed: 19627506]
12. Pagano L, Caira M, Valentini CG, Posteraro B, Fianchi L. Current Therapeutic Approaches to Fungal Infections in Immunocompromised Hematological Patients. Blood Rev. 2010; 24:51–61. [PubMed: 20056300]
13. Brown GD, Denning DW, Levitz SM. Tackling Human Fungal Infections. Science. 2012; 336:647. [PubMed: 22582229]
14. Sudbery P, Gow N, Berman J. The Distinct Morphogenic States of *Candida albicans*. Trends Microbiol. 2004; 12:317–324. [PubMed: 15223059]

15. Slavin MA, Sorrell TC, Marriott D, Thursky KA, Nguyen Q, Ellis DH, Morrissey CO, Chen SCA, Dis ASI. Candidaemia in Adult Cancer Patients: Risks for Fluconazole-Resistant Isolates and Death. J. Antimicrob. Chemother. 2010; 65:1042–1051. [PubMed: 20202987]
16. Dimopoulos G, Karabinis A, Samonis G, Falagas ME. Candidemia In Immunocompromised and Immunocompetent Critically Ill Patients: A Prospective Comparative Study. Eur. J. Clin. Microbiol. 2007; 26:377–384.
17. Lark RL, Chenoweth C, Saint S, Zemencuk JK, Lipsky BA, Plorde JJ. Four Year Prospective Evaluation Of Nosocomial Bacteremia: Epidemiology, Microbiology, and Patient Outcome. Diagn. Microbiol. Infect. Dis. 2000; 38:131–140. [PubMed: 11109010]
18. Fazly A, Jain C, Dehner AC, Issi L, Lilly EA, Ali A, Cao H, Fidel PL Jr. Rao RP, Kaufman PD. Chemical Screening Identifies Filastatin, A Small Molecule Inhibitor of *Candida Albicans* Adhesion, Morphogenesis, And Pathogenesis. Proc. Natl. Acad. Sci. U.S.A. 2013; 110:13594–13599. [PubMed: 23904484]
19. Jones T, Federspiel NA, Chibana H, Dungan J, Kalman S, Magee BB, Newport G, Thorstenson YR, Agabian N, Magee PT, et al. The Diploid Genome Sequence of *Candida albicans*. Proc. Natl. Acad. Sci. U.S.A. 2004; 101:7329–7334. [PubMed: 15123810]
20. Netea MG, Brown GD, Kullberg BJ, Gow NA. An Integrated Model of the Recognition of *Candida Albicans* by the Innate Immune System. Nat. Rev. Microbiol. 2008; 6:67–78. [PubMed: 18079743]
21. Karlsson AJ, Pomerantz WC, Weisblum B, Gellman SH, Palecek SP. Antifungal Activity from 14-Helical Beta-Peptides. J. Am. Chem. Soc. 2006; 128:12630–12631. [PubMed: 17002340]
22. Netea MG, Gow NA, Munro CA, Bates S, Collins C, Ferwerda G, Hobson RP, Bertram G, Hughes HB, Jansen T, et al. Immune Sensing of *Candida Albicans* Requires Cooperative Recognition of Mannans and Glucans by Lectin and Toll-like Receptors. J. Clin. Invest. 2006; 116:1642–1650. [PubMed: 16710478]
23. Sudbery PE. Growth of *Candida albicans* Hyphae. Nat. Rev. Microbiol. 2011; 9:737–748. [PubMed: 21844880]
24. Claudon P, Violette A, Lamour K, Decossas M, Fournel S, Heurtault B, Godet J, Mely Y, Jamart-Gregoire B, Averlant-Petit MC, Briand JP, et al. Consequences of Isostructural Main-Chain Modifications for the Design of Antimicrobial Foldamers: Helical Mimics of Host-Defense Peptides Based on a Heterogeneous Amide/Urea Backbone. Angew. Chem., Int. Ed. 2010; 49:333–336.
25. Spanu T, Posteraro B, Fiori B, D'Inzeo T, Campoli S, Ruggeri A, Tumbarello M, Canu G, Trecarichi EM, Parisi G, et al. Direct MALDI-TOF Mass Spectrometry Assay of Blood Culture Broths for Rapid Identification of Candida Species Causing Bloodstream Infections: An Observational Study in Two Large Microbiology Laboratories. J. Clin. Microbiol. 2012; 50:176–179. [PubMed: 22090401]
26. Heil EL, Daniels LM, Long DM, Rodino KG, Weber DJ, Miller MB. Impact of a Rapid Peptide Nucleic Acid Fluorescence *in Situ* Hybridization Assay on Treatment Of Candida Infections. Am. J. Health-Syst. Pharm. 2012; 69:1910–1914. [PubMed: 23111676]
27. Fernandez J, Erstad BL, Petty W, Nix DE. Time to Positive Culture and Identification for Candida Blood Stream Infections. Diagn. Microbiol. Infect. Dis. 2009; 64:402–407. [PubMed: 19446982]
28. Nguyen MH, Wissel MC, Shields RK, Salomoni MA, Hao BH, Press EG, Shields RM, Cheng SJ, Mitsani D, Vadnerkar A, et al. Performance of Candida Real-time Polymerase Chain Reaction, beta-D-Glucan Assay, and Blood Cultures in the Diagnosis of Invasive Candidiasis. Clin. Infect. Dis. 2012; 54:1240–1248. [PubMed: 22431804]
29. Koo S, Bryar JM, Page JH, Baden LR, Marty FM. Diagnostic Performance of the (1f3)-beta-D-Glucan Assay for Invasive Fungal Disease. Clin. Infect. Dis. 2009; 49:1650–1659. [PubMed: 19863452]
30. Yang Q, Su QP, Wang GY, Wen DZ, Zhang YH, Bao HZ, Wang L. Production of Hybrid Phage Displaying Secreted Aspartyl Proteinase Epitope of *Candida Albicans* and Its Application for the Diagnosis of Disseminated Candidiasis. Mycoses. 2007; 50:165–171. [PubMed: 17472610]
31. Morrison CJ, Hurst SF, Reiss E. Competitive Binding Inhibition Enzyme-Linked Immunosorbent Assay That Uses the Secreted Aspartyl Proteinase of *Candida albicans* as an Antigenic Marker for

Diagnosis of Disseminated Candidiasis. Clin. Diagn. Lab. Immunol. 2003; 10:835–848. [PubMed: 12965914]

32. Macdonald F, Odds FC. Purified *Candida-albicans* Proteinase in the Serological Diagnosis of Systemic Candidosis. J. Am. Chem. Soc. 1980; 243:2409–2411.
33. Naglik JR, Challacombe SJ, Hube B. *Candida albicans* Secreted Aspartyl Proteinases in Virulence and Pathogenesis. Microbiol. Mol. Biol. Rev. 2003; 67:400–428. [PubMed: 12966142]
34. Avni T, Leibovici L, Paul M. PCR Diagnosis of Invasive Candidiasis: Systematic Review and Meta-Analysis. J. Clin. Microbiol. 2011; 49:665–670. [PubMed: 21106797]
35. Cassone A. Development of Vaccines for Candida albicans: Fighting a Skilled Transformer. Nat. Rev. Microbiol. 2013; 11:884–891. [PubMed: 24232568]
36. Poulain D. *Candida albicans*, Plasticity and Pathogenesis. Crit. Rev. Microbiol. 2013 10.3109/1040841X.2013.813904.
37. Mao CB, Liu A, Cao B. Virus-Based Chemical and Biological Sensing. Angew. Chem., Int. Ed. 2009; 48:6790–6810.
38. Liu A, Abbineni G, Mao CB. Nanocomposite Films Assembled from Genetically Engineered Filamentous Viruses and Gold Nanoparticles: Nanoarchitecture- and Humidity-Tunable Surface Plasmon Resonance Spectra. Adv. Mater. 2009; 21:1001–1005.
39. Ghosh D, Lee Y, Thomas S, Kohli AG, Yun DS, Belcher AM, Kelly KA. M13-Templated Magnetic Nanoparticles for Targeted *in Vivo* Imaging of Prostate Cancer. Nat. Nanotechnol. 2012; 7:677–682. [PubMed: 22983492]
40. Smith GP, Petrenko VA. Phage Display. Chem. Rev. 1997; 97:391–410. [PubMed: 11848876]
41. Chen X, Scala G, Quinto I, Liu W, Chun TW, Justement JS, Cohen OJ, vanCott TC, Iwanicki M, Lewis MG, et al. Protection of Rhesus Macaques Against Disease Progression From Pathogenic SHIV-89.6PD by Vaccination with Phage-Displayed HIV-1 Epitopes. Nat. Med. 2001; 7:1225–1231. [PubMed: 11689887]
42. Petrenko VA, Smith GP, Gong X, Quinn T. A Library of Organic Landscapes on Filamentous Phage. Protein Eng. 1996; 9:797–801. [PubMed: 8888146]
43. Lee JH, Domaille DW, Cha JN. Amplified Protein Detection and Identification through DNA-Conjugated M13 Bacteriophage. ACS Nano. 2012; 6:5621–5626. [PubMed: 22587008]
44. Wittenberg NJ, Haynes CL. Using Nanoparticles to Push the Limits of Detection. Wires Nanomed. Nanobiol. 2009; 1:237–254.
45. Massart R. Preparation of Aqueous Magnetic Liquids in Alkaline and Acidic Media. IEEE Trans. Magn. 1981; 17:1247–1248.
46. Cao BR, Mao CB. Identification of Microtubule-Binding Domains on Microtubule-Associated Proteins by Major Coat Phage Display Technique. Biomacromolecules. 2009; 10:555–564. [PubMed: 19186939]
47. Perera K, Murray A. Development of an Indirect ELISA for the Detection of Serum Igg Antibodies Against Region IV of Phase 1 Flagellin Of Salmonella Enterica Serovar Brandenburg in Sheep. J. Med. Microbiol. 2009; 58:1576–1581. [PubMed: 19696151]
48. Yuan L, Giovanni M, Xie J, Fan C, Leong DT. Ultrasensitive IgG Quantification Using DNA Nano-Pyramids. NPG Asia Mater. 2014; 6:e112.
49. Lerner MB, D'Souza J, Pazina T, Dailey J, Goldsmith BR, Robinson MK, Johnson ATC. Hybrids of a Genetically Engineered Antibody and a Carbon Nanotube Transistor for Detection of Prostate Cancer Biomarkers. ACS Nano. 2012; 6:5143–5149. [PubMed: 22575126]
50. Abbineni G, Modali S, Safiejko-Mroczka B, Petrenko VA, Mao CB. Evolutionary Selection of New Breast Cancer Cell-Targeting Peptides and Phages with the Cell-Targeting Peptides Fully Displayed on the Major Coatand Their Effects on Actin Dynamics during Cell Internalization. Mol. Pharmaceutics. 2010; 7:1629–42.
51. Ma K, Wang DD, Lin Y, Wang J, Petrenko V, Mao CB. Synergetic Targeted Delivery of Sleeping-Beauty Transposon System to Mesenchymal Stem Cells Using LPD Nanoparticles Modified with a Phage-Displayed Targeting Peptide. Adv. Funct. Mater. 2013; 23:1172–1181. [PubMed: 23885226]
52. Ghadjari A, Matthews RC, Burnie JP. Epitope Mapping *Candida Albicans* Proteinase (SAP 2). FEMS Immunol. Med. Microbiol. 1997; 19:115–123. [PubMed: 9395056]

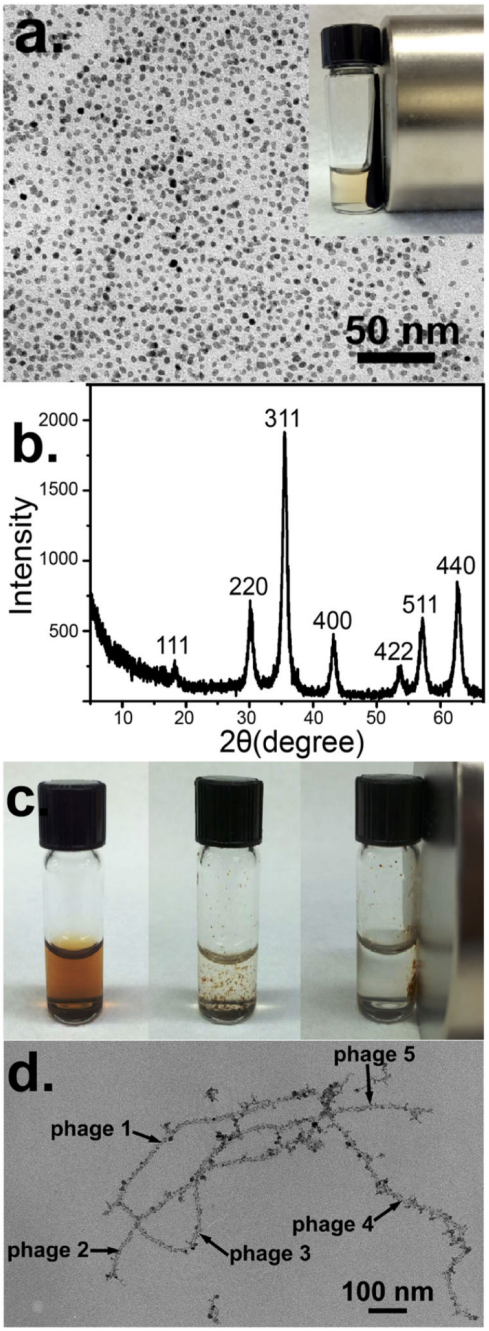

Figure 1.

TEM image (a) and XRD pattern (b) of the synthesized MNPs. The inset in (a) shows the attraction of MNPs toward a magnet. (c) Photographs showing MNPs solution (left) and the mixture of MNPs and PK-ASIT-phage (where ASIT-MNP-phage complexes were formed) in the absence (middle) and presence (right) of a magnet. (d) TEM image of the ASIT-MNP-phage complexes shown in (c).

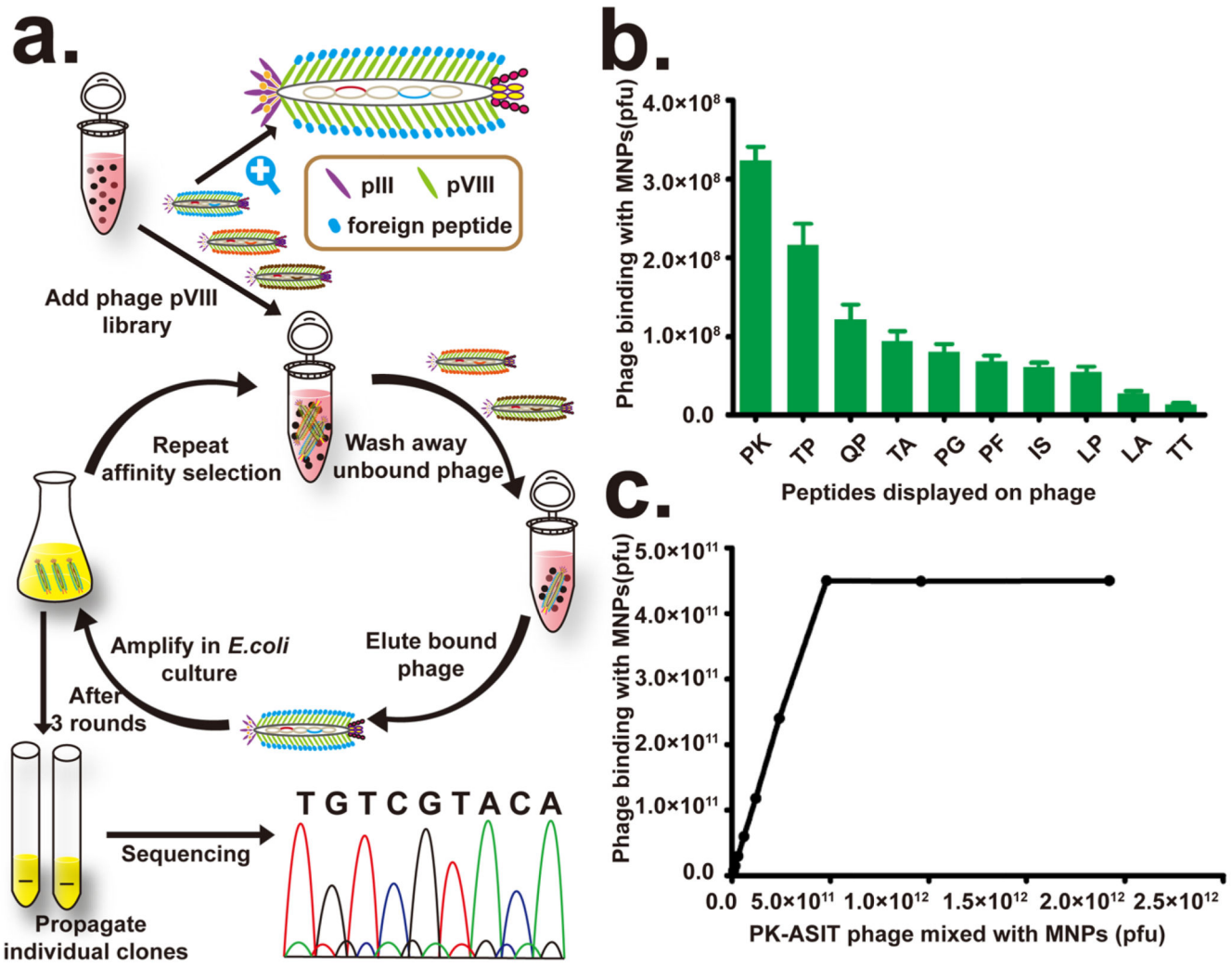

Figure 2.

Schematic of affinity-selection of MNPs-binding phages (a) and the binding ability of selected phage to MNPs (b and c). (b) Affinity-binding test of selected phages. The amount of phage (input) added to interact with excess MNPs was 3.5×10^8 pfu and the amount of output (eluted phage) was shown in the plot for phages displaying different peptides. The results indicate that the phage displaying PK peptide has the strongest affinity to MNPs. PK = PTYSLVPRLATQPFK; TP = TWVASALKNLLYACP; QP = QLPSSTPLYATTWQP; TA = TVSDEVRLLRLPSTA; PG = PSATERLPAQSHPEG; PF = PFISYGAQTPLLPVF; IS = IRQTRSRTRLSRWAS; LP = LRTSPSKQRDHLTSP; LA = LALSPQSWPGPANSA; TT = TPPSSSLVVLQSKAT. (c) Binding tests between MNPs and PK-ASIT-phage. The results show that the maximum amount of PK-ASIT-phage for binding with 100 μg MNPs is 4.5×10^{11} pfu.

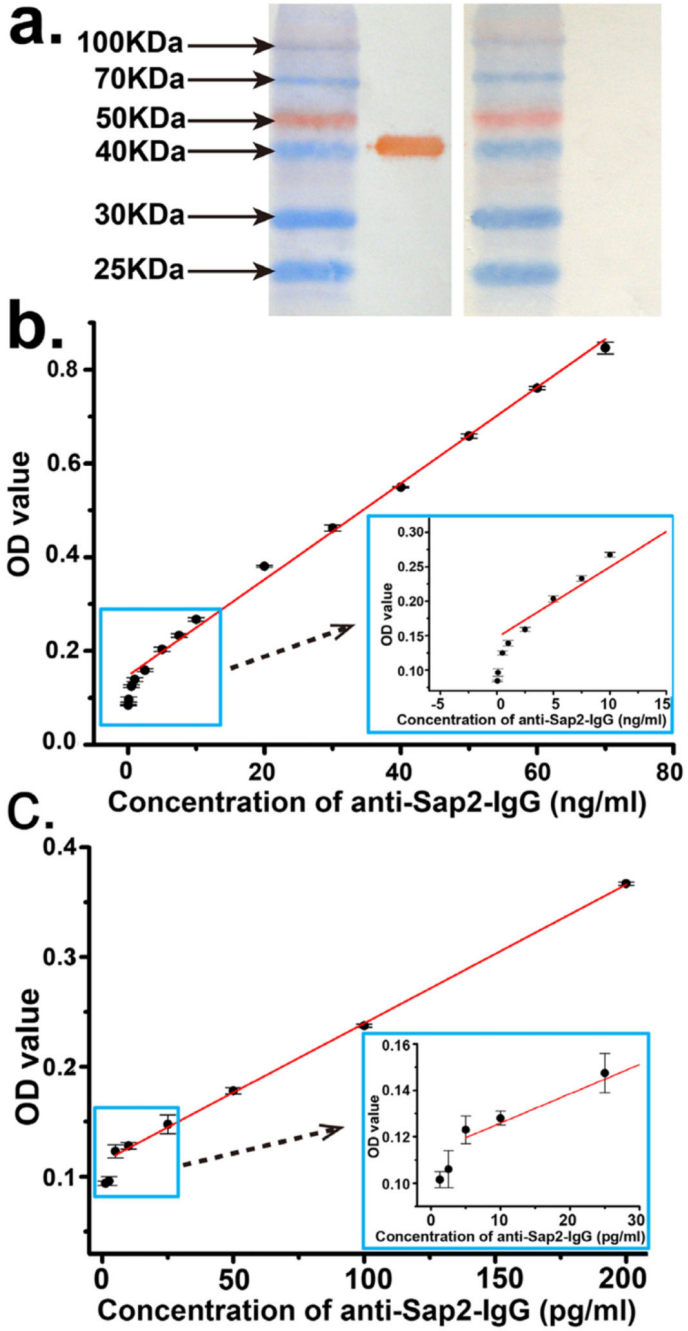

Figure 3.

(a) Western blot analysis showing the specificity of ASIT-MNP-phage for detecting anti-Sap2-IgG in the serum of cancer patients. The data was generated by two steps: First, recombinant Sap2 (rSap2) proteins were run on two SDS-PAGE gels and then transferred onto nitrocellulose membranes. Second, the nitrocellulose membranes with rSap2 proteins were divided into two groups, which were incubated with the eluted antibodies collected from serum of patients and healthy control, respectively. Left image: left lane, marker; right lane, serum from *Candida albicans*-infected cancer patients. Right image: left lane, marker;

right lane, serum from healthy control. (b) Correlation between the ELISA signal (optical density at 450 nm) and the predetermined concentration of anti-Sap2-IgG in rSap2 protein-based ELISA method (control). (c) Correlation between the ELISA signal and the predetermined concentration of anti-Sap2-IgG in ASIT-MNP-phage-based ELISA method.

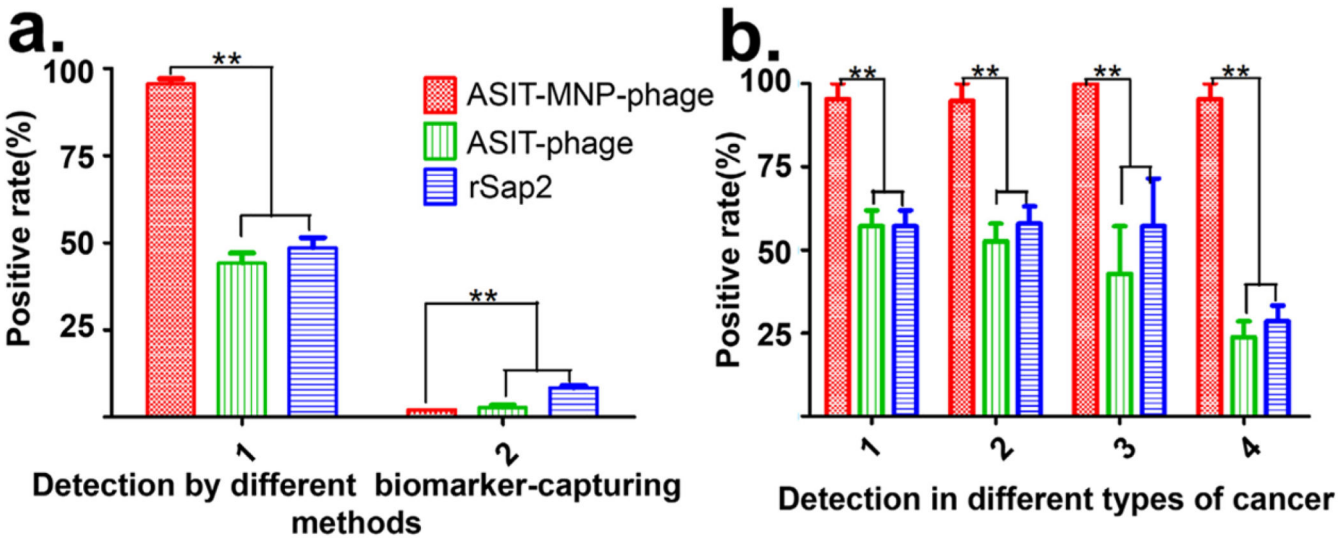

Figure 4.

Detection of anti-Sap2-IgG in sera of cancer patients with *C. albicans* infection. (a) The percentage of anti-Sap2-IgG positive population among all patients detected using different assays. 1, *C. albicans*-infected patients; 2, healthy control. Each data point represents the mean for 3 independent experiments ± SD. (b) The percentage of anti-Sap2-IgG positive population among patients of each specific cancer type: 1, lung cancer; 2, breast cancer; 3, intestinal cancer; 4, other cancers. Each data point represents the mean for 3 independent experiments ± SD, $^{**}p < 0.01$. Both a and b share the same legends as shown in (a).

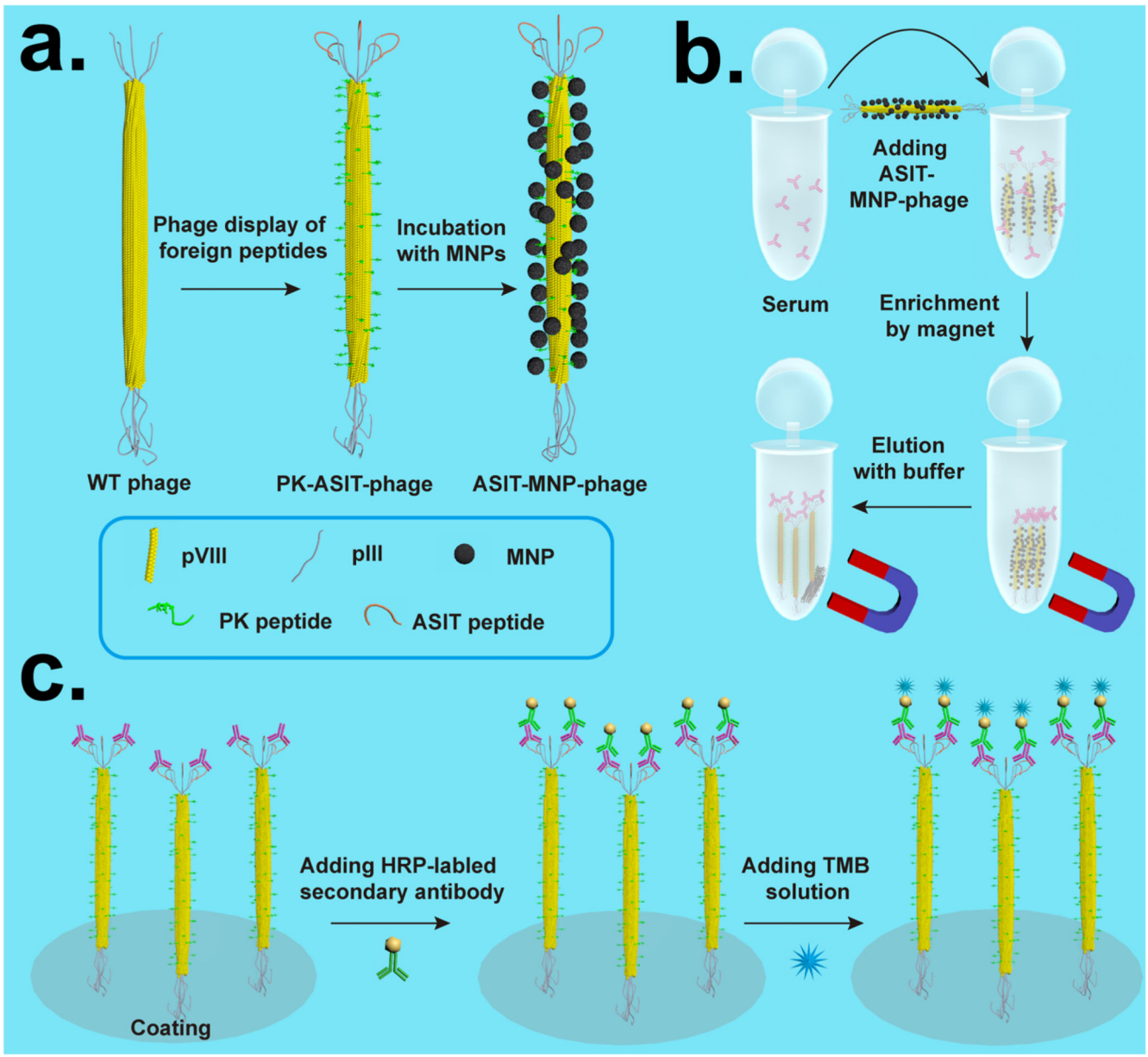

Scheme 1.

Schematic of using ASIT-MNP-phage for the detection of anti-Sap2-IgG from human serum. (a) Two peptides were double-displayed on the surface of wild type (WT) phage, with MNP-binding peptide displayed on the pVIII (major coat protein on the side wall) and anti-Sap2-IgG-binding peptide displayed on the pIII (minor coat protein at the tip). MNPs were then bound to the side wall of the resultant phage due to the display of MNP-binding peptides on the major coat, forming ASIT-MNP-phage complex. (b) ASIT-MNP-phage was added to the human sera and captured the biomarker (anti-Sap2-IgG) through its pIII tip. A magnet was then used to enrich the complex of ASIT-MNP-phage and the biomarker. An elution buffer was then used to elute the ASIT-phage/biomarker complex from the MNPs. (c) The eluted ASIT-phage/biomarker complex was coated on the ELISA plate, followed by

the addition of horseradish peroxidase (HRP)-labeled secondary antibody that recognized the biomarker. A 3, 3′, 5, 5′-tetramethylbenzidine (TMB) coloring solution was further added to the resultant complex to develop color for the detection of the biomarker. PK denotes MNP-binding peptide (PTYSLVPRLATQPFK). ASIT denotes anti-Sap2-IgG-targeting peptide (VKYTS). It should be noted that the viral nanofibers are not necessarily vertically oriented on the surface of the plates and the current cartoon is only meant to easily highlight the binding event between viral nanofibers, target antibodies and secondary antibodies.

TABLE 1

The Number of Total *C. albicans*-Infected Patients and the Average Number of Cases Detected by Different Assays (Healthy Population Was Used as a Control)

		Anti-Sap2 positive population		
	population	**ASIT-MNP-phage**	**ASIT-phage**	**rSap2**
Cancer patients with infection	68	65 ± 1	30 ± 2	33 ± 2
Healthy people	144	3	4 ± 1	12 ± 1

TABLE 2

The Number of *C. albicans*-Infected Patients with Different Cancer Types and the Average Number of Cases Detected by Different Assays[a]

		Anti-Sap2 positive population		
	population	**ASIT-MNP-phage**	**ASIT-phage**	**rSap2**
Lung cancer	21	20 ± 1	12 ± 1	12 ± 1
Breast cancer	19	18 ± 1	10 ± 1	11 ± 1
Intestinal	7	7	3 ± 1	4 ± 1
Others	21	20 ± 1	5 ± 1	6 ± 1

[a]The ASIT-MNP-phage method identified more candidiasis patients for each cancer type. Systemic *C. albicans* infection was confirmed positive by blood culture.